SUPPLEMENTARY DATA

CCR2-deficiency in monocytes impairs angiogenesis and functional recovery after ischemic stroke in mice

Jordi Pedragosa[1,2], Francesc Miró-Mur[2,3], Amaia Otxoa-de-Amezaga[1,2], Carles Justicia[1,2], Francisca Ruíz-Jaén[1,2], Peter Ponsaerts[4], Manolis Pasparakis[5], and Anna M. Planas[1,2,*]

[1] Department of Brain Ischemia and Neurodegeneration, Institut d'Investigacions Biomèdiques de Barcelona (IIBB), Consejo Superior de Investigaciones Científicas (CSIC), Barcelona, Spain

[2] Area of Neurociences, Institut d'Investigacions Biomèdiques August Pi i Sunyer (IDIBAPS), Barcelona, Spain

[3] Fundació Clínic, Barcelona, Spain

[4] Laboratory of Experimental Hematology, University of Antwerp, Antwerp, Belgium

[5] CECAD Research Center, Institute for Genetics, University of Cologne, Cologne, Germany

Corresponding author:

Anna M. Planas, PhD
IIBB-CSIC, IDIBAPS,
Rosselló 161, planta 6,
08036-Barcelona, Spain.
e-mail: anna.planas@iibb.csic.es
Tel: +34-93 363 83 27

Supplementary Table S1. List of primer sequences for PCR

Gene	Taqman ID Assay	Accession no.	Amplicon lenght (bp)	Exon boundary
Acta2	Mm01546133_m1	NM_007392.3	88	Exon 1-2
Activin1	Mm00434339_m1	NM_008380.1	65	Exon 2-3
Areg	Mm01354339_m1	NM_009704.3	142	Exon 5-6
Arg1	Mm00475988_m1	NM_007482.3	65	Exon 1-2
Bdnf	Mm04230607_s1	NM_001048139.1	92	Exon 2-2
Ccl2	Mm00441242_m1	NM_011333.3	74	Exon 1-2
Ccr2	Mm00438270_m1	NM_009915.2	100	Exon 2-3
Chil3	Mm00657889_mH	NM_009892.2	90	N/A
Csf2	Mm01290062_m1	NM_009969.4	125	Exon 2-3
Egfr	Mm01187858_m1	NM_007912.4	101	Exon 2-3
Fgf2	Mm01285715_m1	NM_008006.2	119	Exon 2-3
Flk1	Mm01222421_m1	NM_010612.2	64	Exon 13-14
Flt1	Mm00438980_m1	NM_010228.3	59	Exon 15-16
Flt4	Mm01292604_m1	NM_008029.3	72	Exon 12-13
Gapdh	Mm99999915_g1	NM_001289726.1	107	Exon 2-3
Hprt1	Mm00446968_m1	NM_013556.2	65	Exon 6-7
Il10	Mm00439614_m1	NM_010548.2	79	Exon 1-2
Il1b	Mm00434228_m1	NM_008361.3	90	Exon 3-4
Il6	Mm00446190_m1	NM_031168.2	78	Exon 2-3
Mmp2	Mm00439498_m1	NM_008610.2	62	Exon 2-3
Mmp3	Mm00440295_m1	NM_010809.1	66	Exon 4-5
Mmp9	Mm00442991_m1	NM_013599.3	76	Exon 12-13
Nos2	Mm00440502_m1	NM_010927.3	66	Exon 21-22
Reg3b	Mm00440616_g1	NM_011036.1	73	Exon 5-6
Tmem119	Mm00525305_m1	NM_146162.2	72	Exon 1-2
Tnfa	Mm00443258_m1	NM_013693.3	81	Exon 1-2
Vegfa	Mm00437306_m1	NM_001025250.3	61	Exon 3-4
Vegfc	Mm00437310_m1	NM_009506.2	78	Exon 1-2

Gene	SYBR green Primer sequence 5' - 3'	Accession no.	Amplicon lenght (bp)	Exon boundary
Angpt1	F: 5'-GGAACCGAGCCTACTCACAG-3' R: 5'-CGAACCACCAACCTCCTGTT-3'	NM_009640.4	204	Exon 7 Exon 8-9
Angpt2	F: 5'-AGTCAGGACTCACCACCAGT-3' R: 5'-GCCATCTTCTCGGTGTTGGA-3'	NM_007426.4	128	Exon 5 Exon 6
Gfap	F: 5'-AAGGTCCGCTTCCTGGAA-3' R: 5'-GGCTCGAAGCTGGTTCAGTT-3'	NM_010277.3	63	Exon 1 Exon 1
Igf1	F: 5'-GTGGACCGAGGGGCTTTTACTTC-3' R: 5'-TTTGCAGCTTCGTTTTCTTGTTTG-3'	NM_010512.5	246	Exon 1-2 Exon 3-4
Il23a	F: 5'-GACCCACAAGGACTCAAGGAC-3' R: 5'- ATGGGGCTATCAGGGAGTAGAG-3'	NM_031252.2	131	Exon 2 Exon 3
Pdgfb	F: 5'-TTGAACATGACCCGAGCACA-3' R: 5'-AGATGGGCTTCTTTCGCACA-3'	NM_011057.4	310	Exon 3 Exon 5
Pdgfbr	F: 5'-AGGAGTGATACCAGCTTTAGTCC-3' R: 5'-CCGAGCAGGTCAGAACAAAGG-3'	NM_008809.2	152	Exon 2 Exon 3
Rpl14	F: 5'-GGCTTTAGTGGATGGACCCT-3' R: 5'-ATTGATATCCGCCTTCTCCC-3'	NM_025974.2	143	Exon 3 Exon 4
Tgfb1	F: 5'-TGCTTCAGCTCCACAGAGAA-3' R: 5'-TACTGTGTGTCCAGGCTCCA-3'	NM_011577.2	155	Exon 5-6 Exon 6

Supplementary Figure S1

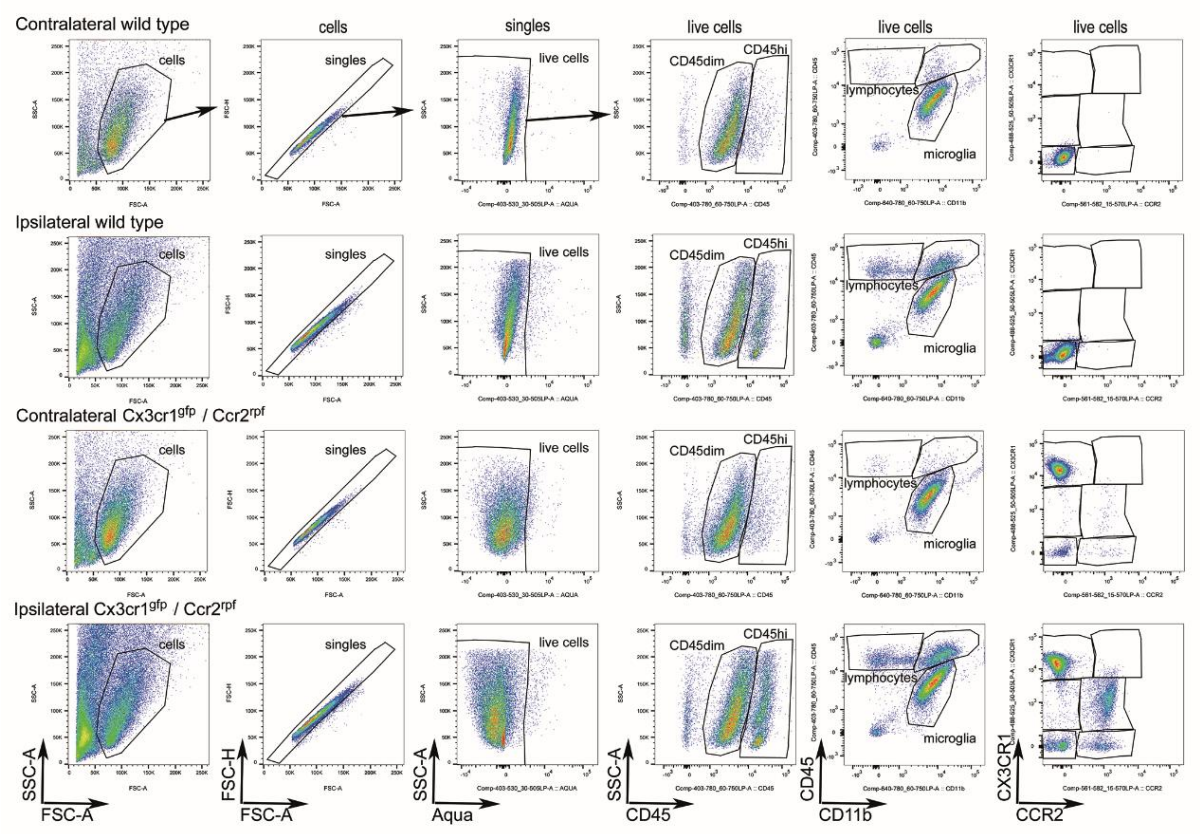

Supplementary Fig. S1 Gating strategy to identify the different cell populations expressing CCR2^{rfp} and/or CX3CR1^{gfp} in the ischemic brain tissue of Ccr2$^{rfp/+}$Cx3cr1$^{gfp/+}$ transgenic mice. We studied the contralateral and ipsilateral (ischemic) cerebral cortex of wild type mice and double-transgenic Ccr2$^{rfp/+}$Cx3cr1$^{gfp/+}$ mice 4 days post-ischemia. CD45^{hi} cells increase in the ipsilateral vs. the contralateral hemisphere. GFP^{+} cells (CX3CR1) cells and RFP^{+} (CCR2) cells are not seen in the wild type mice. Ccr2$^{rfp/+}$Cx3cr1$^{gfp/+}$ mice show CX3CR1-gfp^{hi} microglia in the contralateral and ipsilateral hemisphere. In addition, other CX3CR1-gfp^{+} cells and/or CCR2-rfp^{+} cells become apparent in the ipsilateral hemisphere.

Supplementary Figure S2

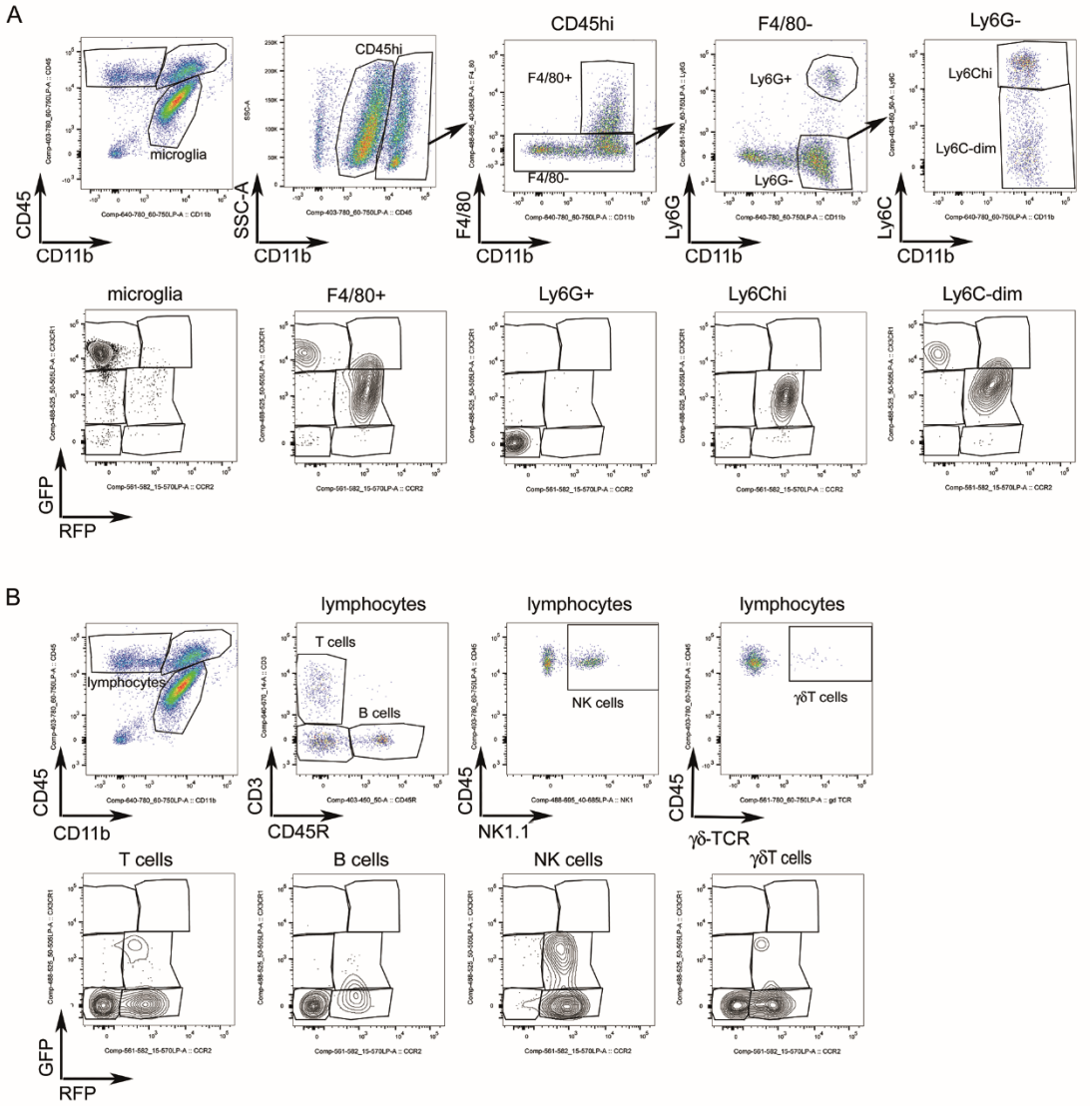

Supplementary Fig. S2. CCR2 and CX3CR1 expression in different cells subsets as assessed with GFP and RFP fluorescence. Following gating in Supplementary Fig 1, GFP and RFP fluorescence in the ischemic brain tissue (4 days post-ischemia) is shown in the gates of: A) myeloid cells, including microglia, F4/80 macrophages, neutrophils ($Ly6G^{+}$), and monocytes ($Ly6G^{-}$ $Ly6C^{+}$); B) lymphocytes, including B and T cells, NKs cells and γδ-TCR cells. Microglia are GFP^{hi}; $F4/80^{+}$ macrophages are RFP^{+} GFP^{+}; $Ly6G^{+}$ neutrophils are RFP^{-} GFP^{-}; and $Ly6C^{+}$ monocytes show different degrees of RFP and GFP. Lymphocytes show major subsets of $CCR2^{+}$ RFP^{+} cells and a few $CX3CR1^{+}$ GFP^{+} cells.

Supplementary Figure S3

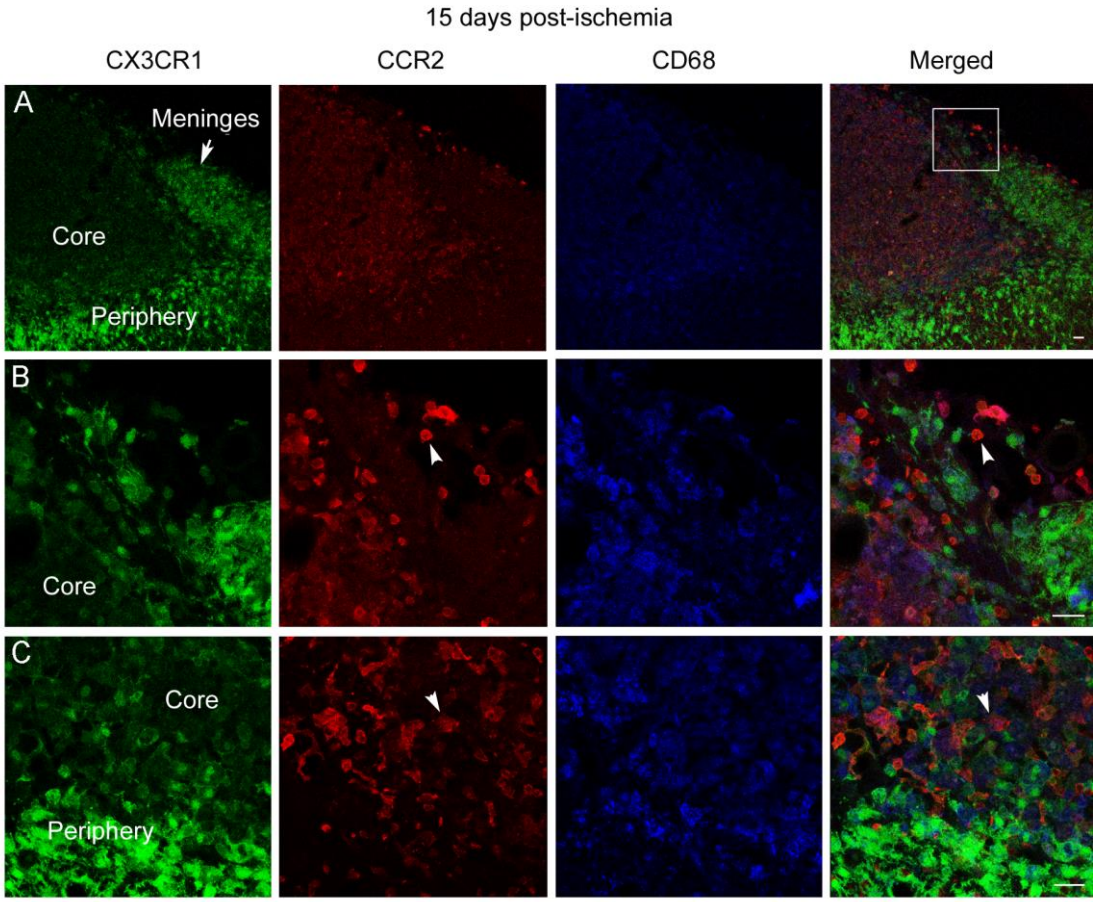

Supplementary Fig. S3. Infiltrating leukocytes 15 days post-ischemia. Subpopulations of leukocytes infiltrating the ischemic brain tissue at day 15 in $Ccr2^{rfp/+}Cx3cr1^{gfp/+}$ mice (n=3). A dense layer of very bright gfp^{+} microglia (green) surrounds and clearly delimitates the ischemic core, which is packed with high density of cells with rfp fluorescence (red), gfp^{low}, and positive for CD68 (blue). Microglial cells are located at the border of the lesion. They show large cell bodies with short and thick ramifications. Infiltrating small, round, and very bright rfp^{+} leukocytes are prominent within the core of the lesion, at the interface between the infarcted core and also within the peripheral microglial layer, and at the leptomeninges. Scale bar= 20 µm.

Supplementary Figure. S4

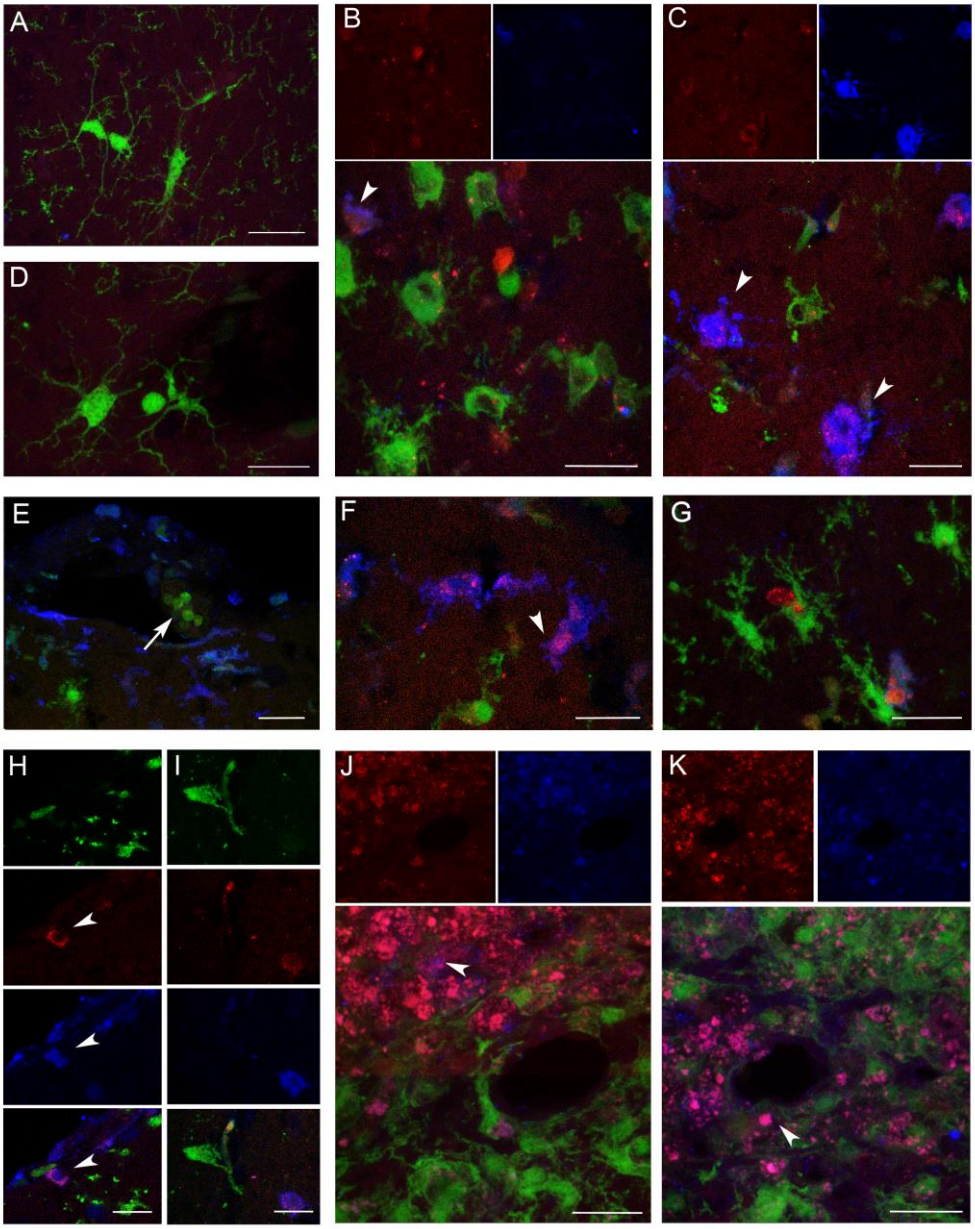

Supplementary Fig. S4. Subsets of infiltrating monocytes, but not microglia, express Arginase-1. Expression of Arg1 (blue) in the $Ccr2^{rfp/+}Cx3cr1^{gfp/+}$ transgenic mice 4 days (A-I) and 15 days (J-K) post-ischemia. Microglial ($CX3CR1^{hi}$, intense green fluorescence) cells do not express Arg1, neither in the control tissue (A) nor at the periphery of the lesion (D). In the border (B) and core (C-I) of the lesion, Arg1 immunoreactivity is detected in RFP^+ cells (red, arrowheads), whereas most GFP^+ cells do not express Arg1 (arrows). At 15 days $Arg1^+$ cells are found in the core of the lesion in cells expressing RFP (J-K). Scale bar: 20 μm.

Supplementary Figure S5

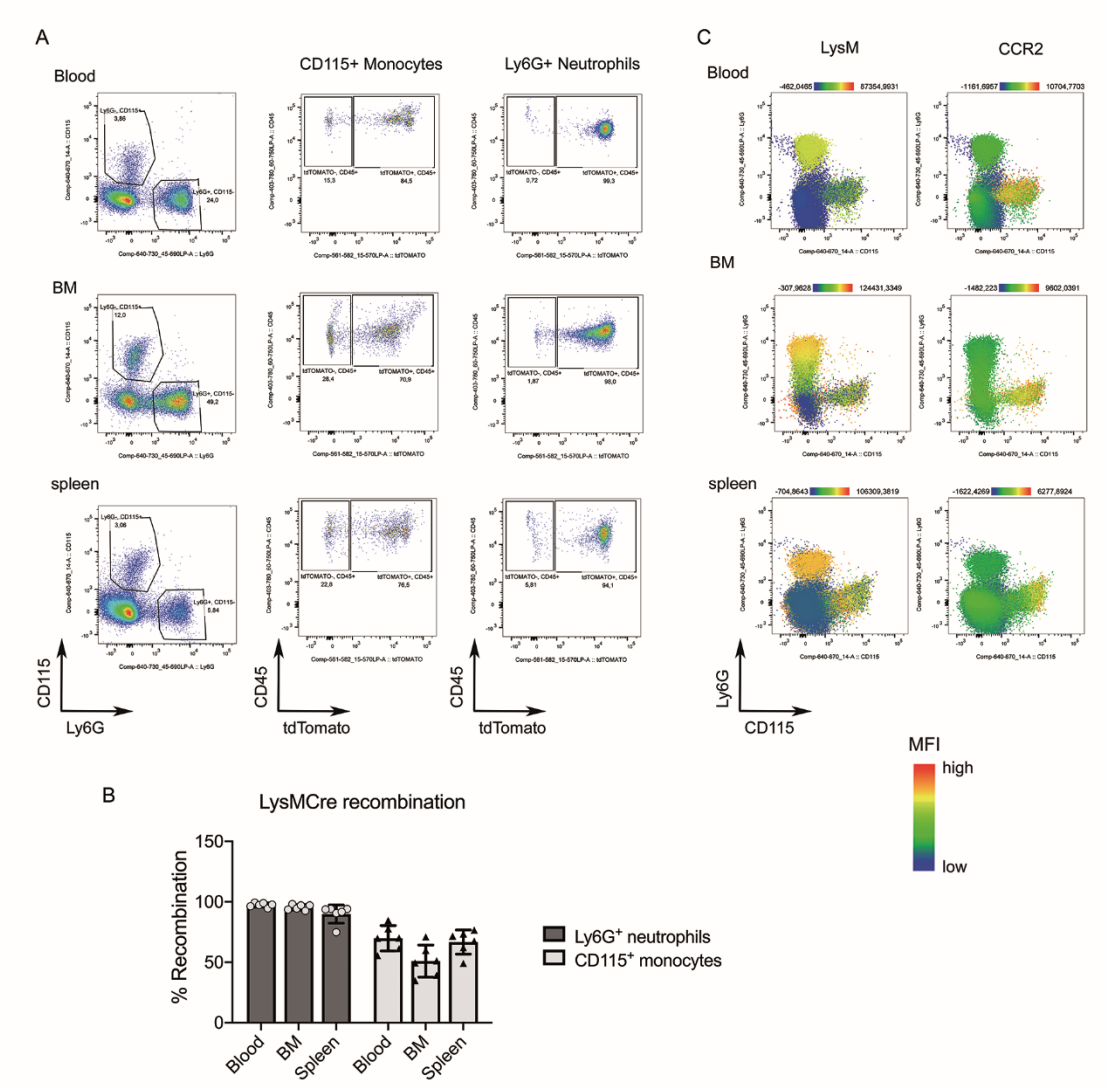

Supplementary Fig. S5. Cre-recombination and CCR2 expression in different myeloid cells as assessed in LysMcre:Rosa26-tdT mice. A) Gating strategy to assess the efficiency of LysMcre recombination in monocytes ($CD115^+$) and neutrophils ($Ly6G^+$) of LysMcre:Rosa26-tdT mice in blood, bone marrow (BM) and spleen. B) Quantification of LysMcre recombination in monocytes and neutrophils in the above organs (n=6). C) In spite of very high LysMcre-recombination in $Ly6G^+$ neutrophils, the expression of CCR2 in these cells is very low. In contrast, CCR2 expression is high in monocytes. Color code indicates the value of mean fluorescence intensity (MFI).

Supplementary Figure S6

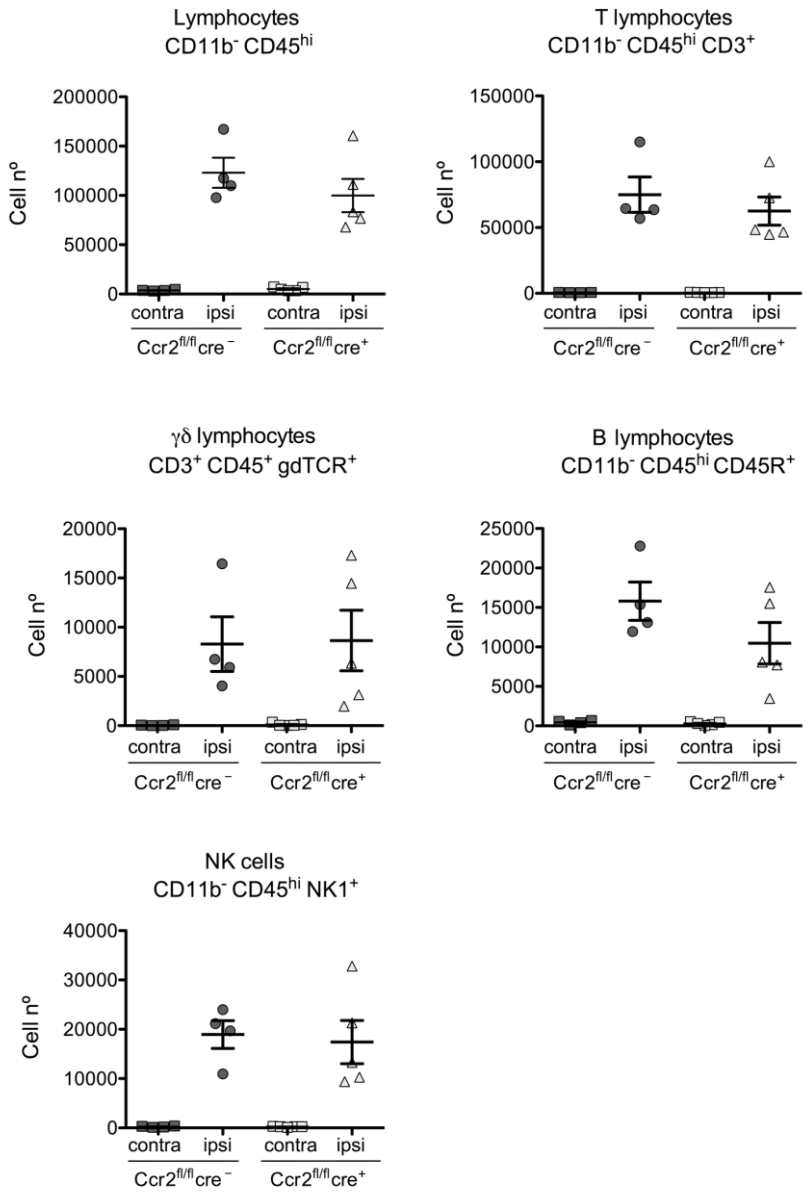

Supplementary Fig. S6. Cell counts for infiltrating lymphoid cells in the brain tissue one-day post-ischemia in mice with CCR2-deficient monocytes and controls. Ischemia was induced in littermate $Ccr2^{fl/fl}LysMcre^{+}$ mice (mice with CCR2-deficient monocytes, n=5) and $Ccr2^{fl/fl}LysMcre^{-}$ mice (control genotype, n=4) and the contralateral (contra) and ipsilateral (ipsi, ischemic) cerebral cortex was studied 1 day later by flow cytometry. Graphs show absolute cell numbers for the different lymphoid cell populations. Lymphocytes infiltrate the ipsilateral brain hemisphere after ischemia but we found no statistically significant differences between genotypes (Two-way ANOVA by genotype and brain region).

Supplementary Figure S7

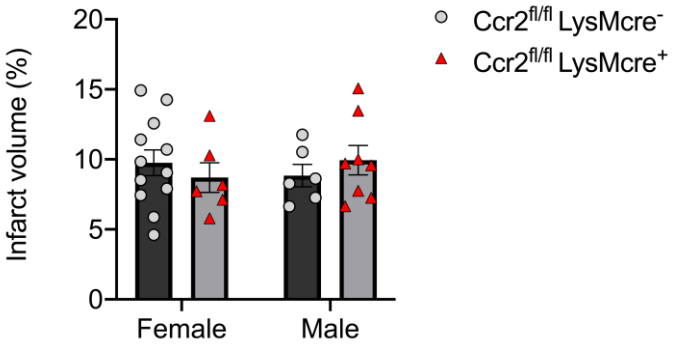

Supplementary Fig. S7. No sex or genotype differences in infarct volume 15 days post-ischemia. We analyzed whether infarct volume (%) was different as a function of sex (n=18 female and n=14 male) and genotype (n=18 $Ccr2^{fl/fl}LysMcre^{-}$ and n= 14 $Ccr2^{fl/fl}LysMcre^{+}$) by two-way ANOVA. There were no statistically significant differences between groups: sex effect p=0.878, genotype effect p=0.987, with no interaction p=0.313.

Supplementary Figure S8

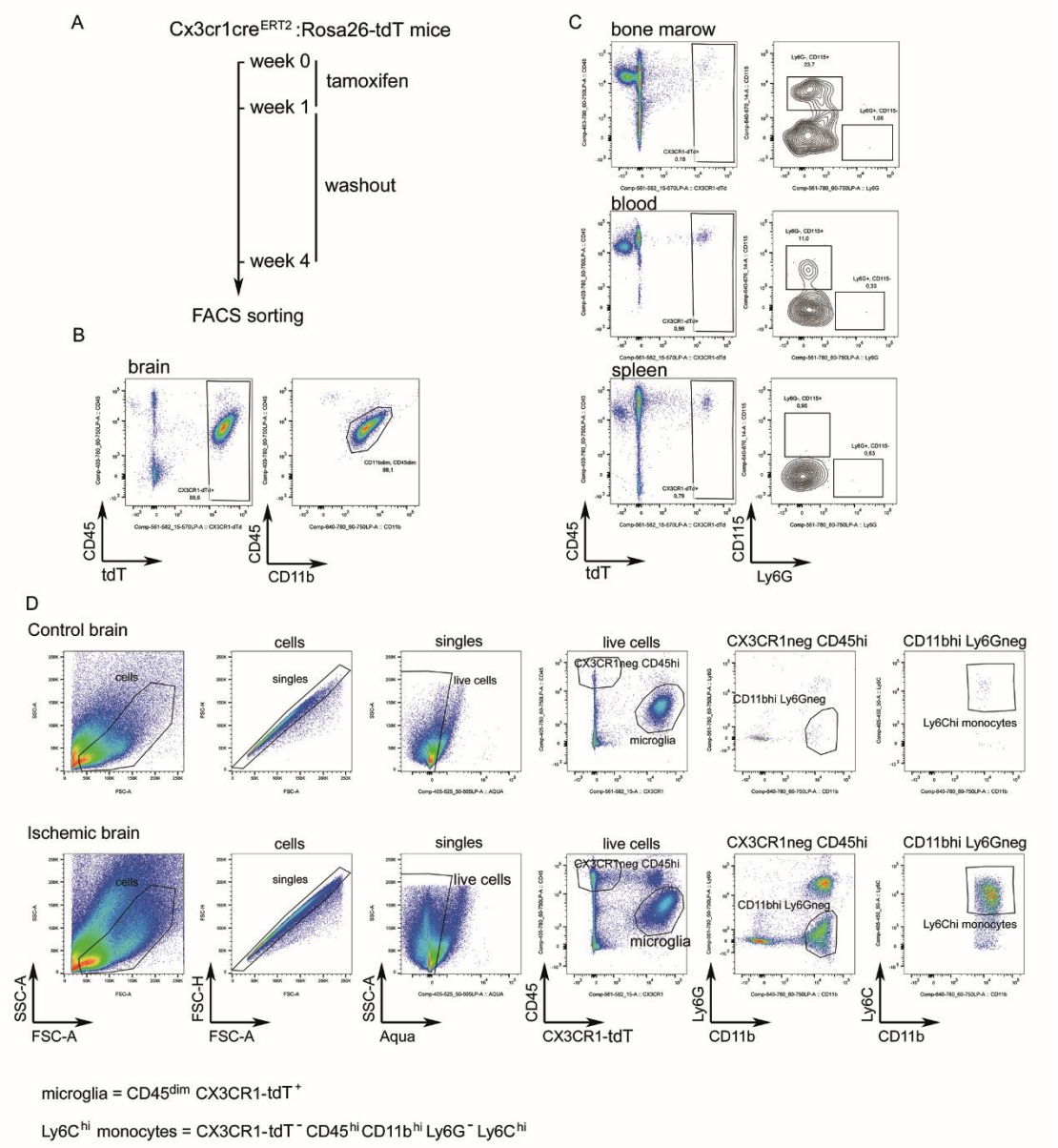

Supplementary Fig. S8. Strategy for FACS cell sorting microglia and Ly6C^{hi} monocytes. A) We used Cx3cr1cre^{ERT2}:Rosa26-tdT mice that received tamoxifen during one week, followed by 3 weeks of washout prior to induction of ischemia and FACS cell sorting at day 1. B) Flow cytometry plots showing that all red fluorescent (tdT) cells of the ischemic brain are CD11b^{dim}CD45^{dim} microglial cells (99.1%). C) Very few tdT^{+} cells (<1%) are detected in the bone marrow, blood and spleen, and the gates for monocytes (CD115^{+}) and neutrophils (Ly6G^{+}) show absence of tdT^{+} cells. D) Sorting strategy from the ischemic and control brain tissue for microglia (CD45^{dim} Cx3cr1-tdT^{+} cells), and Ly6C^{hi} monocytes (CX3CR1-tdT^{negative} CD45^{hi} CD11b^{hi} Ly6G^{negative} Ly6C^{hi}).